LAND SUBSIDENCE MONITORING AND ANALYSIS IN FUZHOU BASED ON INSAR AND MULTISPECTRAL REMOTE SENSING TECHNOLOGY

Y. Y. Zhu [1], Y. F. He [1,2] *, H. Y. Li [1], Z. P. Lv [1,3], G. C. Xu[1]

[1] Institute of Space Science and Applied Technology, Harbin Institute of Technology (Shenzhen), Shenzhen 518055, China –
zhuyuyan123@gmail.com; heyufang0823@163.com; lihanyu608608@163.com; lvzhiping@hit.edu.cn; xuguochang@hit.edu.cn;
[2] GFZ German Research Centre for Geosciences, Department of Geodesy, Section of Remote Sensing, 14473 Potsdam –
heyufang0823@163.com;
[3] Institute of Geospatial Information, Information Engineering University, Zhengzhou 450052, China - lvzhiping@hit.edu.cn.

Commission III, WG III/3

KEY WORDS: Land Subsidence, InSAR, Fuzhou, Multispectral, Time series.

ABSTRACT:

Interferometric Synthetic Aperture Radar (InSAR) technology has millimeter level measurement accuracy and has great advantages in urban land subsidence monitoring. Meanwhile, multispectral remote sensing technique can also provide a large amount of urban features changes information for analyzing the causes of land subsidence. In this study, SAR and multispectral images are both used to monitor and analyze land subsidence in Fuzhou of China. 115 scenes Sentinel-1 SAR images from May 2017 to May 2021 are used based on the Persistent Scatterers Interferometric (PSI) method to evaluate the land subsidence in Fuzhou, while Sentinel-2 multispectral images are used to evaluate several remote sensing indexes. During SAR data processing, Generic Atmospheric Correction Online Service for InSAR (GACOS) data is used to remove atmospheric errors for higher accuracy land subsidence. In order to analyze the relationship between the land subsidence and land cover changes in urban areas, the Soil-Adjusted Vegetation Index (SAVI), Normalized Difference Built-up Index (NDBI) and Modified Normalized Difference Water Index (MNDWI) of the main subsidence areas are obtained based on Sentinel-2 multispectral images from 2016 to 2021. In the end, it is found that the land subsidence in some areas exceeded 12 mm/year in Fuzhou. The time series of four areas with severe subsidence were analyzed, and the cumulative subsidence reached about 60 mm. Besides, the spatial distribution and temporal changes of vegetation, buildings and water bodies in these areas were obtained based on the multispectral data, it is found there is very less relationship between the land subsidence and the urban features. It is concluded that that the main causes of the land subsidence are the changes of land internal components such as groundwater and others.

1. INTRODUCTION

According to statistics from the United Nations, there are more than 4 billion people living in urban areas in the world currently, and the number of people lived in urban areas are still increasing (Ritchie and Roser, 2018). Urbanization has the advantages of promoting economic growth and regional development (Bai et al., 2014), and land subsidence is an important issue in this process (Wang et al., 2018). According to a survey using 2003–2010 ENVISAT C-band SAR archive, the land subsidence of the Eastern Trans-Mexican Volcanic Belt, Mexico is analyzed. The vertical subsidence rates is up to −53 mm/year within the city of Puebla (Cigna et al., 2019). Rome Metropolitan Area is also suffering from land subsidence geohazard (Delgado et al., 2019). In China, Beijing is developing rapidly and the maximum subsidence rate is 140.01 mm/year (Luo et al., 2018). Therefore, urban land subsidence monitoring is very urgent recently.

Fuzhou is the capital of Fujian Province, China and it also faces the problem of land subsidence. It is a city with a total area of 11,968 square kilometres, a built-up area of 416 square kilometers, and a permanent population of 8.42 million. The previous monitoring of Fuzhou subsidence showed that there are subsidence points, and many of them have caused damage to buildings and other facilities (Lan et al., 2019). Therefore, it is necessary to use the InSAR method to evaluate the recent land subsidence in Fuzhou. At the same time, multispectral remote sensing data can be used to obtain surface information of cities such as building changes and so on, thus the subsidence areas

acquired by InSAR can be analyzed again with multispectral data to obtain surface information of these areas.

Synthetic Aperture Radar Interferometry (InSAR) technology is a technology that can be used for large-scale ground deformation monitoring (Massonnet and Feigl, 1998). Sentinel-1, ALOS-1 and ENVISAT data are used to observe land subsidence in Wuhan, China (Hu et al., 2022). Envisat ASAR C-band data, ALOS-1 PALSAR L-band SAR, Sentinel-1 C-band and ALOS-2 PALSAR L-band are used to obtain land subsidence in a metropolitan in Maceió, Brazil (Vassileva et al., 2021). And another research use 2007-2010 ENVISAT, ALOS-1 data, and 2017-2020 Sentinel-1 data study the ground displacement in Taiyuan basin (Tang et al., 2021). And a research based on Sentinel-1 InSAR find the land subsidence through the Iran and also get the high resolution land subsidence in Tehran and Mashhad (Haghighi and Motagh, 2021). However, there is no monitoring of subsidence in Fuzhou in 2020 using SAR data.

Multispectral remote sensing technique can be used to detect the land cover changes, which can extract information including vegetation, building, water and so on. Multispectral remote sensing are used to obtain information on urban vegetation on Temuco, Chile and assessed the potentiality of design of a green corridors system (Moreno et al., 2020). Gaofen-1 multispectral data are used and a remote sensing index are improved to obtain higher-precision urban building information (Bai et al., 2020). Landsat data are used to obtained the relationship between Normalized Difference Water Index (NDWI) index and surface

---

* Corresponding author

temperature in Raipur, India, and the impact of different seasons on this relationship are analyzed (Guha et al., 2020). However, these studies often only use remote sensing indices to analyze the information of the entire urban area. These studies did not use InSAR to obtain the results of urban deformation, and then focused on the analysis of deformation areas using remote sensing indices.

In this study, the Persistent Scatterers InSAR (PS-InSAR) method is used based on the Sentinel-1 data from 2017 to 2021 combined to monitor the land subsidence in Fuzhou. It is a very effective method to monitor the land deformation by permanent scatterers (Ferretti et al., 2001). At the same time, the SAVI, MNDWI and NDBI indices of the subsidence area were obtained by using Sentinel-2 data, and the changes of the optical remote sensing index in the subsidence area were also analyzed combined with InSAR subsidence.

2. STUDY AREA AND DATA

2.1 Study Area

Figure 1 shows the location of Fuzhou (25°16′ N–26°39′ N, 118° 08′ E–120°31′ E) and its surrounding urban areas. It is the capital of Fujian Province, located at the eastern end of the central part of Fujian Province, on the west coast of the Taiwan Strait. Most of the area is located in the Fuzhou Basin, at the mouth of the lower reaches of the Min River. The north and west are medium and low mountains, which slope from the southwest to the east, and the terrain is relatively complex. The natural environment of Fuzhou is transitional. It belongs to the subtropical marine monsoon climate with abundant rainfall. The annual average temperature is 19.6℃, the annual average relative humidity is 77%, the annual average sunshine is 1888h, and the annual frost-free period is 326 days.
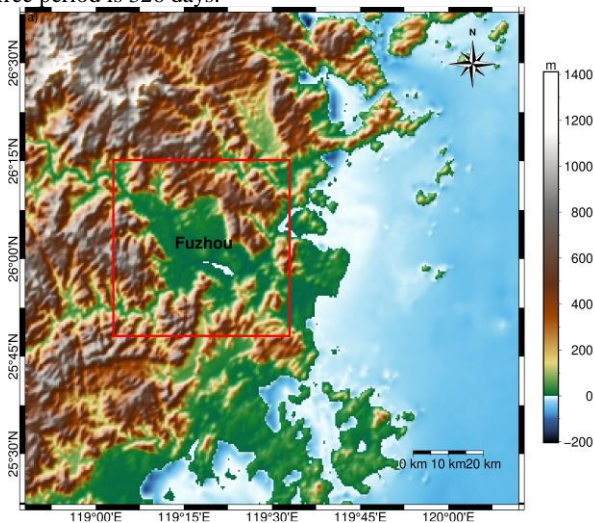

Figure 1. Geographical and topographic information of the study area, located in the Fuzhou Basin.

Fuzhou is the largest industrial city in Fujian Province, as well as the political, economic and cultural center of the province. From 1996 to 2005, the urban area of Fuzhou has been expanding rapidly, and the type of land used for the underlying surface of the main urban area has undergone tremendous changes (Yanhong et al., 2020). Historical data shows that land subsidence has existed in Fuzhou since the 1990s. Recent observations show that by the end of 2017, there were still multiple subsidence funnels in Fuzhou, which may be related to

the construction of subways and urban roads (Hu et al., 2019). We choose the area A, area B, area C and area D to obtain the detail information. The name of these areas are Jin'an District, Cangshan District, Nantong town and Shanggan town, respectively.

2.2 Data

The data used is from the Sentinel-1A satellite, which was launched in 2014 as part of ESA's Copernicus program. It is a C-band Synthetic Aperture Radar (SAR) imaging satellite operating in a near-polar sun-synchronous orbit at an altitude of about 697 km with a revisit period of 12 days (Geudtner et al., 2014). 115 images from May 2017 to May 2021 is used in this study. SRTM data with a spatial resolution of 30 meters is used as the external DEM data (Farr et al., 2007).

Sentinel-2 multispectral images are used in this study (Drusch et al., 2012). However, Fuzhou belongs to the monsoon climate region, which has a lot of cloudiness in summer, so it is difficult to obtain high-quality images for remote sensing index calculation. These images covered by cloud are removed, which is done in Google Earth Engine (GEE) (Gorelick et al., 2017).

3. METHOD

In this study, Sentinel-1 SAR images and Sentinel-2 multispectral images were processed separately. Figure 2 is the flowchart of the methods used in the study.

3.1 InSAR Method

The whole SAR data process is mainly divided into two steps. The first step is performed in the SeNtinel Application platform (SNAP) software, which generates an interferogram for each image paired with the center image from the Single Look Complex (SLC) data. Afterwards, PS-InSAR processing is performed in the Stanford Method on Persistent Scatterers (StaMPS) software, which generates the deformation time series from the interferogram.

Based on the SNAP software, SAR images processing is performed at first. The master image was first selected as the reference image, and all images were registered with it. It requires sub-pixel-level registered images. After that, the swath and burst of the sentinel data were eliminated to obtain images without gaps. Then interferogram were generated by temporal and spatial threshold method. Finally, the flat-ground and topographic phase in the interferogram were removed by applying 30m SRTM DEM. Then the PS-InSAR method was applied based on the StaMPS, and the PS point with better coherence were selected to monitor the area. And GACOS data was used to reduce atmospheric errors (Yu et al., 2018). Finally, the time series deformation results of the entire Fuzhou region were obtained.

3.2 Multispectral Method

The main subsidence areas were also analyzed using multispectral data, which were directly processed using GEE. In GEE, the built-in function is used to retrieve the time series data of the study area, and the retrieved data from Dec. 2015 to Dec. 2021 have a time resolution of 6 days. Then we use the function of GEE for clipping. Due to the high cloud cover in summer, the cloud cover metadata provided by GEE was used to remove the cloud. The processed images have a resolution of approximately 6 days, and the data is averaged for a monthly composite of the

processing. Then the SAVI, NDBI and MNDWI functions are defined, which are used to obtain various remote sensing indices of the study area in batches.
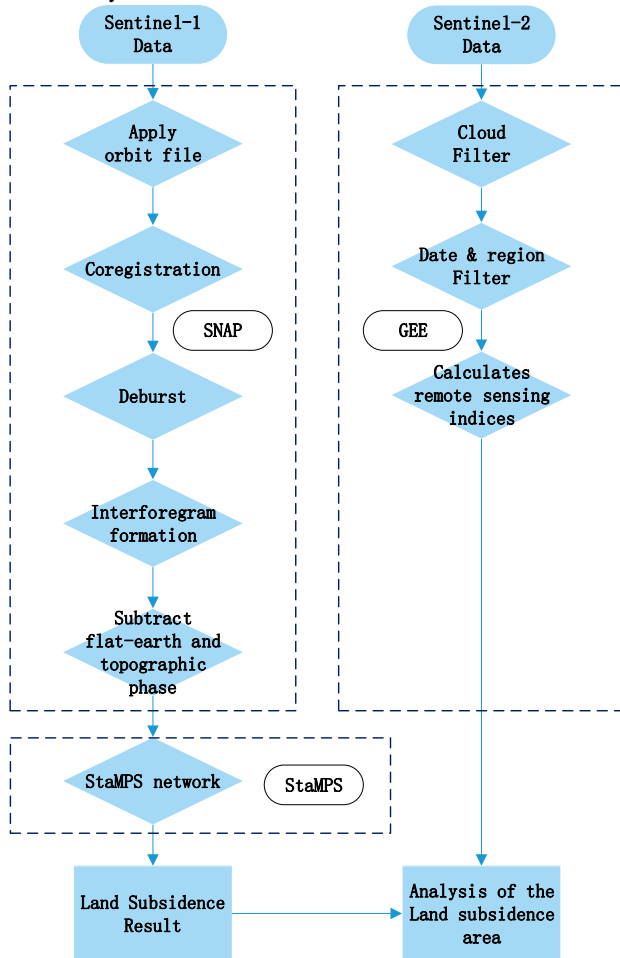

Figure 2. Flowchart of the method in the study.

The equation for $SAVI$ is this:

$$SAVI = \frac{(NIR-Red)\times(1+L)}{NIR+Red+L},\qquad(1)$$

where NIR = near infrared band
   Red = red band
   L = soil adjustment index
Here NIR is band8 of Sentinel-2 images, Red is band4 of Sentinel-2 images and L uses 0.2.

The equation for $NDBI$ is this:

$$NDBI = \frac{SWIR-NIR}{SWIR+NIR},\qquad(2)$$

where $SWIR$= short-wave infrared band
   NIR = near infrared band
Here $SWIR$ is band11 of Sentinel-2 images, NIR is band8 of Sentinel-2 images.

The equation for $MNDWI$ is this:

$$MNDWI = \frac{Green-MIR}{Green+MIR},\qquad(3)$$

where $Green$= green band
   MIR = Mid-infrared band

Here $Green$ is band3 of Sentinel-2 images, MIR is band11 of Sentinel-2 images.

4. RESULTS AND DISCUSSION

In this section, we will show the land subsidence result of the entire Fuzhou area, and then analyze several areas with severe subsidence. First, the subsidence time series results are analyzed, and then the multispectral remote sensing index time series of these areas are obtained. Figure 3 shows the land subsidence rate in Fuzhou from May 2017 to May 2021.
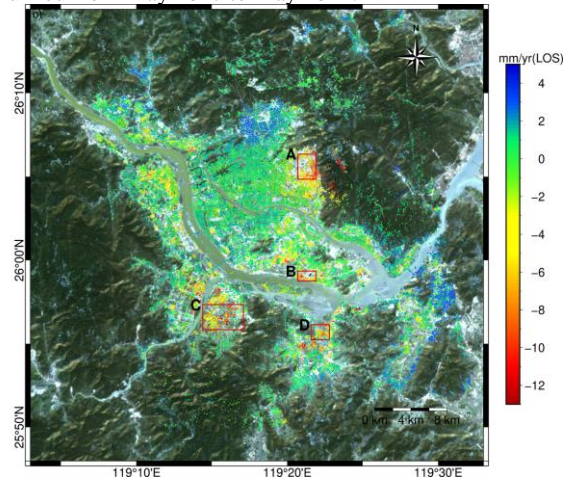

Figure 3. Land subsidence rate in the line of sight (LOS) direction of Fuzhou from May 2017 to May 2021. And the areas in the four red boxes are areas with relatively serious subsidence.

4.1 Subsidence of The Fuzhou Area

It is found that there is the surface subsidence greater than 10 mm/year in some areas of Fuzhou. The most serious areas have a subsidence rate of more than 12 mm/year, four areas of which are selected for detailed analysis.

Figure 4-a shows the annual average subsidence rate in the northern mountainous area of Fuzhou (Jin'an District), it is found that annual average deformation rate reaches 7.5 mm/year. It is also found that the cumulative subsidence reaches 37.8 mm for one PS point selected in the subsidence area A in Figure 4-b, and the cumulative subsidence of time series changes linearly.

Figure 4-c shows the annual average subsidence rate of the area B near the airport (Cangshan District). The annual average deformation rate of the first phase reached 26.4 mm/year and the annual average deformation rate of the second phase reached 15.6 mm/year. It is found that the cumulative subsidence of area B has two different stages of change curve in Figure 4-d. There is about 35.5 mm cumulative land subsidence occurred from June 2017 to June 2018 in the first phase, and then it is changed to about 41 mm of land subsidence in August 2018 until 2021 In June. According to the multispectral imagery, it is found that the land subsidence is caused by building construction in this area. Besides, this may be due to poor coherence caused by large ground changes during construction.

In the area C (Nantong town), the main subsidence area is located on one side of the river, and adjacent to the subsidence area is a field of farmland. Figure 4-e shows that the annual average subsidence rate of area C ranges from 4 to 12 mm in LOS direction. The cumulative deformation in LOS direction in this

area reaches 40.5 mm in Figure 4-f. The area D is surrounded by rivers on three sides. Figure 4-g shows that the annual average subsidence rate of area D (Shanggan town) ranges from 0 to 12 mm in LOS direction. The cumulative deformation in LOS direction in this area reaches 55.7 mm in Figure 4-h. This area is small and concentrated near sites surrounded by rivers, so it may be associated with rivers.
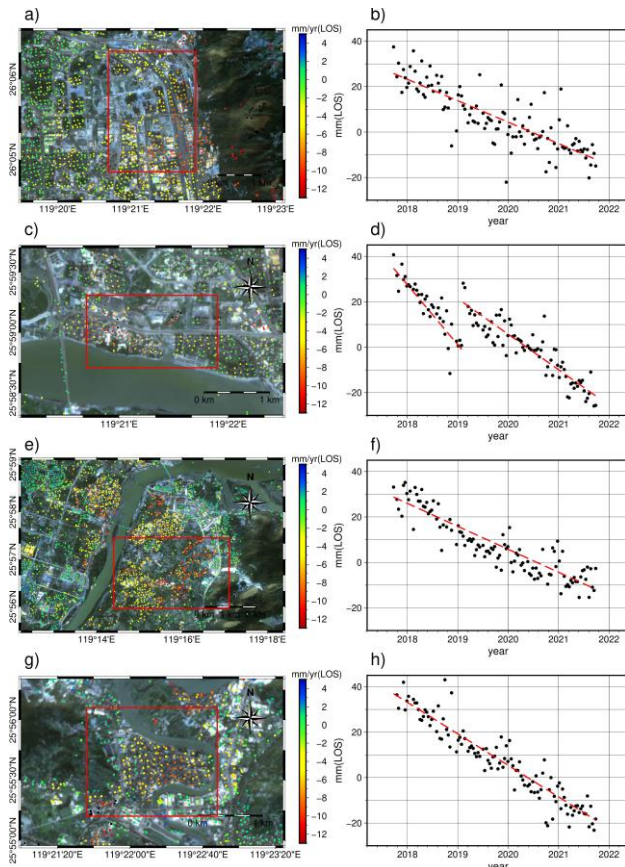

Figure 4. Close up views of four subsidence area. The fig on the right shows the time series in the subsidence areas over time. The red dashed lines are the trend lines of the linear fit.

Compared with other studies, our study has some similarities. TerraSAR-X and leveling data are used in other studies, the difference in the data makes the quality of the results obtained vary. The TerraSAR-X data has a higher resolution, and the leveling data is more accurate, but the time frame of these studies is in 2014 years ago (Lan et al., 2019). Other studies have also used Sentinel-1 data, but most of the data used are before 2019, and most of them are using Small Baseline Subset InSAR (SBAS-InSAR) method (Huang et al., 2019). This method is different from the method in this study in removing atmospheric errors. Some of the subsidence points found in this study are the same as in other studies, which shows the reliability of our research results.

4.2 Results of Multispectral Data

GEE platform is also used to obtain the time series changes of three remote sensing indices of four areas with severe subsidence. Figure 5 shows the remote sensing indices time series of the four areas. Figure 6, Figure 7, Figure 8 and Figure 9 shows the spatial distributed of the remote sensing indices for the main subsidence areas, respectively.
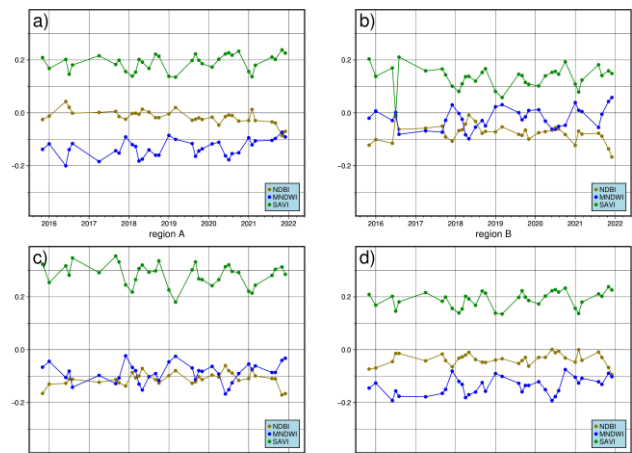

Figure 5. Time series of SAVI、NDBI and MNDWI for the four areas.

According to Figure 5-a, the NDBI value of the area A (Jin'an District) has been around 0 and has decreased slightly. The slight decrease of NDBI value indicates that the building of the area is decreasing. There are some deformation PS points in area A. The building area change will have an impact on the land subsidence. The SAVI level in this area is high, around 0.2, due to the greening in the building. This area does not contain a large body of water and has a low MNDWI value (Figure 6). The results show that building area change causes some land subsidence in urban area.
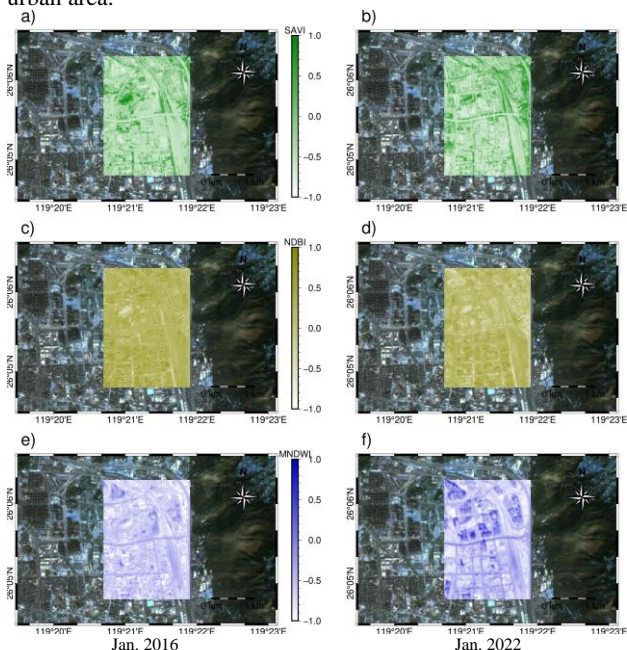

Figure 6. The SAVI, NDBI and MNDWI values of area A at January 2016 and January 2022.

The main components of the area B (Cangshan District) are buildings and roads, so the values and change of SAVI is similar to area A (Figure 5-b). Since there are more water bodies and buildings in this area, the NDBI is smaller than the first area. This can also indicate that there may be construction phenomena, because the NDBI of the construction area is small. At the same time, there are rivers in this area, so MNDWI is larger than area A (Figure 7). This indicates that the surface subsidence obtained from the InSAR results may be related to construction.
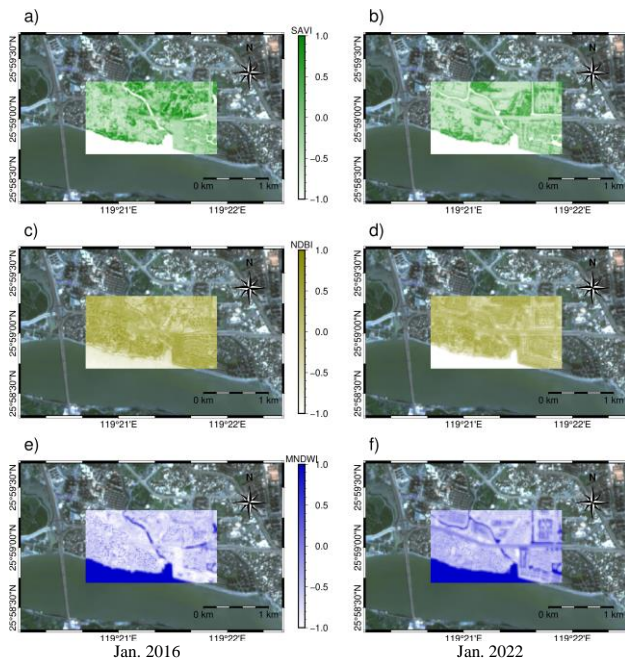
Figure 7. The SAVI, NDBI and MNDWI values of area B at January 2016 and January 2022.

The SAVI of area C (Nantong town) is much larger than that of the other three areas (Figure 5-c), and it can be inferred that this area is a planting area. At the same time, it can still be seen that it has a cyclical fluctuation trend, which also shows that this is a planting area. This is because there are planting and harvesting phenomena in the planting area, and planting areas are often cyclical changes in SAVI. Both NDBI and MNDWI are low in this area, which is in line with the less river and buildings in the area (Figure 8). Combined with the analysis of InSAR results and multispectral results, the cause of surface subsidence in this area may be groundwater extraction caused by agricultural irrigation.
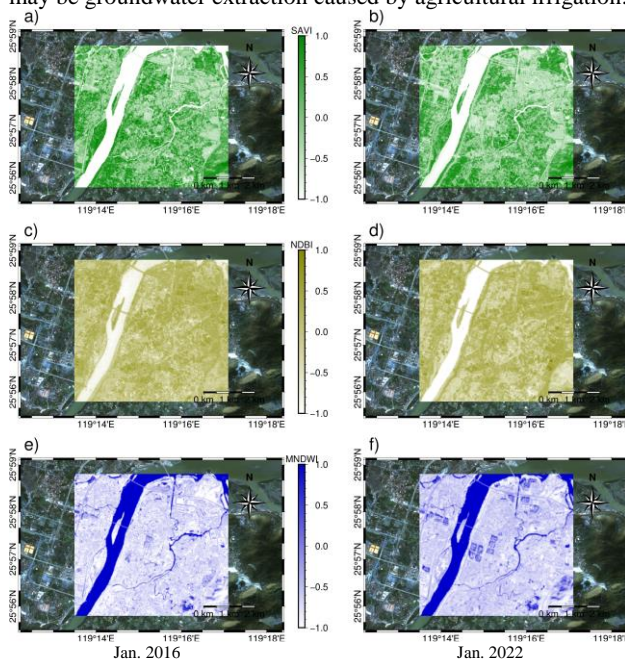

Figure 8. The SAVI, NDBI and MNDWI values of area C at January 2016 and January 2022.

The composition of area D (Shanggan town) is more complex, including rivers, buildings and vegetation. However, the multispectral image shows that the building type is mainly

bungalows, rather than high-rise buildings like other areas (Figure 5-d). Although there are more buildings in this area, the SAVI in this area is higher and the NDBI is lower than area A, which may be caused by the different spectral curves of bungalows and tall buildings (Figure 9). The foundation of the bungalows are less stable than the large buildings, so it may cause land subsidence.
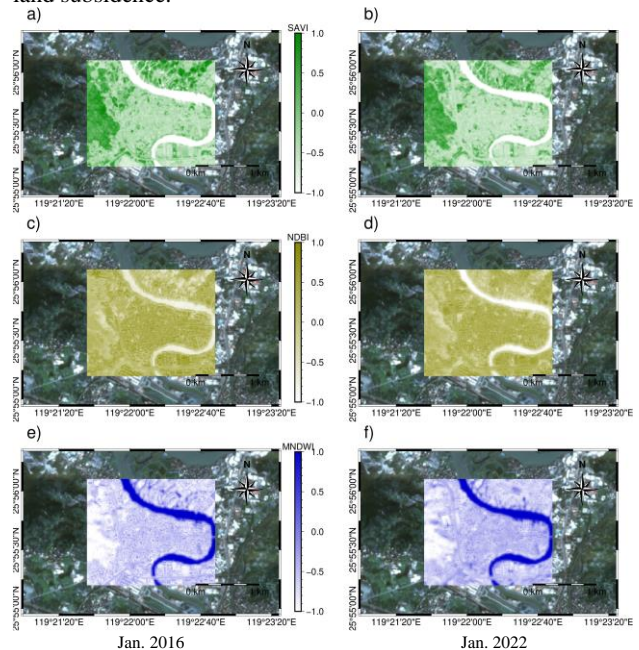

Figure 9. The SAVI, NDBI and MNDWI values of area D at January 2016 and January 2022.

This study shows that the correlation between multispectral data and surface subsidence is weak, but can also be used as a supplement to urban information to obtain information that cannot be obtained by radar. Areas with more buildings tend to have better coherence, and at the same time, people should pay attention to the disasters caused by land subsidence. Regional PS-InSAR has many disadvantages with more vegetation, and there may be subsidence caused by groundwater extraction.

5. CONCLUSION

In this study, the PS-InSAR method was used to obtain the land subsidence of Fuzhou based on the SNAP and StaMPS software. In order to remove the atmospheric phase, GACOS data is used. Then multispectral images are used to obtain land cover change information.

The results show that there are four main subsidence area including Jin'an District, Cangshan District, Nantong town and Shanggan town in Fuzhou. Annual average deformation rate of area A, B, C and D reaches 7.5 mm/year, 26.4 mm/year, 12 mm/year and 11mm/year respectively. The cumulative subsidence reaches 37.8 mm, 34.8mm, 40.5mm and 55.6mm respectively. It is also found that the accumulated subsidence of these subsidence points are very large, which is useful to the prevention of urban disasters. Compared with the results from other researchers, it is found that the main subsidence areas are almost the same, which reflects the reliability of the method. Three remote sensing indices including SAVI, NDBI and MNDWI are obtained. It is found that the vegetation and water body show seasonal periodic changes with time, and the changes of buildings are chaotic, but the change fluctuates little in the long term.

After combining the InSAR land subsidence information and the change values of land cover type, it is found that the buildings area change will affect the deformation results of the area to a certain extent, the change of vegetation will affect the coherence of InSAR PS points and the reliability of deformation information. And the change of surface water area has little impact on the surrounding building objects. However, these results are also related to the low resolution of the data used, which will be further analyzed in more detail in combination with high resolution SAR and optical multispectral images.

ACKNOWLEDGEMENTS

REFERENCES

Bai, X., Shi, P., Liu, Y., 2014. Society: Realizing China's urban dream. *Nature* 509, 158-160.

Bai, Y., He, G., Wang, G., Yang, G., 2020. WE-NDBI-A new index for mapping urban built-up areas from GF-1 WFV images. *Remote Sensing Letters* 11, 407-415.

Cigna, F., Tapete, D., Garduño-Monroy, V.H., Muñiz-Jauregui, J.A., García-Hernández, O.H., Jiménez-Haro, A., 2019. Wide-area InSAR survey of surface deformation in urban areas and geothermal fields in the eastern Trans-Mexican Volcanic Belt, Mexico. *Remote Sensing* 11, 2341.

Delgado, J.M., Foumelis, M., Stewart, C., Hooper, A., 2019. Measuring urban subsidence in the Rome metropolitan area (Italy) with Sentinel-1 SNAP-StaMPS persistent scatterer interferometry. *Remote Sensing* 11, 129.

Drusch, M., Del Bello, U., Carlier, S., Colin, O., Fernandez, V., Gascon, F., Hoersch, B., Isola, C., Laberinti, P., Martimort, P., 2012. Sentinel-2: ESA's optical high-resolution mission for GMES operational services. *Remote sensing of Environment* 120, 25-36.

Farr, T.G., Rosen, P.A., Caro, E., Crippen, R., Duren, R., Hensley, S., Kobrick, M., Paller, M., Rodriguez, E., Roth, L., 2007. The shuttle radar topography mission. *Reviews of geophysics* 45.

Ferretti, A., Prati, C., Rocca, F., 2001. Permanent scatterers in SAR interferometry. *IEEE Transactions on geoscience and remote sensing* 39, 8-20.

Geudtner, D., Torres, R., Snoeij, P., Davidson, M., Rommen, B., 2014. Sentinel-1 system capabilities and applications, *2014 IEEE Geoscience and Remote Sensing Symposium*. IEEE, pp. 1457-1460.

Gorelick, N., Hancher, M., Dixon, M., Ilyushchenko, S., Thau, D., Moore, R., 2017. Google Earth Engine: Planetary-scale geospatial analysis for everyone. *Remote sensing of Environment* 202, 18-27.

Guha, S., Govil, H., Besoya, M., 2020. An investigation on seasonal variability between LST and NDWI in an urban environment using Landsat satellite data. *Geomatics, Natural Hazards and Risk* 11, 1319-1345.

Haghighi, M.H., Motagh, M., 2021. Land Subsidence Hazard in Iran Revealed by Country-Scale Analysis of SENTINEL-1 Insar. *The International Archives of Photogrammetry, Remote Sensing and Spatial Information Sciences* 43, 155-161.

Hu, B., Yang, B., Zhang, X., Chen, X., Wu, Y., 2019. Time-series displacement of land subsidence in Fuzhou downtown, monitored by SBAS-InSAR technique. *Journal of Sensors* 2019.

Hu, J., Motagh, M., Guo, J., Haghighi, M.H., Li, T., Qin, F., Wu, W., 2022. Inferring subsidence characteristics in Wuhan (China) through multitemporal InSAR and hydrogeological analysis. *Engineering Geology*, 106530.

Huang, H., Xue, D., Zhuo, G., Yu, X., Qiao, J., Yang, L., 2019. Monitoring land subsidence in Fuzhou City (China) using the SBAS-InSAR method with Sentinel-1 imagery data, *2019 6th Asia-Pacific Conference on Synthetic Aperture Radar (APSAR)*. IEEE, pp. 1-5.

Lan, H., Meng, Y., Zhang, Y., 2019. Spatiotemporal evolution analysis of land subsidence in Fuzhou city under the influence of complex factors. *Journal of Engineering Geology* 27, 1350-1361.

Luo, X.G., Wang, J., Xu, Z., Zhu, S., Meng, L., Liu, J., Cui, Y., 2018. Dynamic analysis of urban ground subsidence in Beijing based on the permanent scattering insar technology. *Journal of Applied Remote Sensing* 12, 026001.

Massonnet, D., Feigl, K.L., 1998. Radar interferometry and its application to changes in the Earth's surface. *Reviews of geophysics* 36, 441-500.

Moreno, R., Ojeda, N., Azócar, J., Venegas, C., Inostroza, L., 2020. Application of NDVI for identify potentiality of the urban forest for the design of a green corridors system in intermediary cities of Latin America: Case study, Temuco, Chile. *Urban Forestry & Urban Greening* 55, 126821.

Ritchie, H., Roser, M., 2018. Urbanization. *Our world in data*.

Tang, W., Zhao, X., Bi, G., Li, J., Motagh, M., Chen, M., Chen, H., 2021. Investigation of present-day ground displacement in Taiyuan basin by InSAR in the context of interbasin water transfer project, *EGU General Assembly Conference Abstracts*, pp. EGU21-9340.

Vassileva, M., Al-Halbouni, D., Motagh, M., Walter, T.R., Dahm, T., Wetzel, H.-U., 2021. A decade-long silent ground subsidence hazard culminating in a metropolitan disaster in Maceió, Brazil. *Scientific reports* 11, 1-13.

Wang, Z.-F., Cheng, W.-C., Wang, Y.-Q., 2018. Investigation into geohazards during urbanization process of Xi'an, China. *Natural Hazards* 92, 1937-1953.

Yanhong, C., Yuanbin, C., Chuan, T., 2020. Research on temperature effect of urban green space evolution process based on remote sensing——Taking the main urban area of Fuzhou as an example *Journal of Ecology*

Yu, C., Li, Z., Penna, N.T., Crippa, P., 2018. Generic atmospheric correction model for interferometric synthetic

aperture radar observations. *Journal of Geophysical Research: Solid Earth* 123, 9202-9222.